



HAL
open science

Correlating three centuries of historical and geological data for the marine deposit reconstruction of two depositional environments of the French Atlantic coast

Pierre Pouzet, Mohamed Maanan, Sabine Schmidt, Emmanuelle Athimon,
Marc Robin

► To cite this version:

Pierre Pouzet, Mohamed Maanan, Sabine Schmidt, Emmanuelle Athimon, Marc Robin. Correlating three centuries of historical and geological data for the marine deposit reconstruction of two depositional environments of the French Atlantic coast. *Marine Geology*, 2019, 407, pp.181-191. 10.1016/j.margeo.2018.10.014 . hal-01920313

HAL Id: hal-01920313

<https://hal.science/hal-01920313>

Submitted on 9 Jul 2020

HAL is a multi-disciplinary open access archive for the deposit and dissemination of scientific research documents, whether they are published or not. The documents may come from teaching and research institutions in France or abroad, or from public or private research centers.

L'archive ouverte pluridisciplinaire **HAL**, est destinée au dépôt et à la diffusion de documents scientifiques de niveau recherche, publiés ou non, émanant des établissements d'enseignement et de recherche français ou étrangers, des laboratoires publics ou privés.

1 **Correlating three centuries of historical and geological data for the marine deposit**
2 **reconstruction of two depositional environments of the French Atlantic coast**

3
4 Pierre Pouzet¹, Mohamed Maanan^{1*}, Schmidt Sabine², Athimon Emmanuelle^{1,3}, Marc Robin¹

5
6 ¹ Université de Nantes LETG - UMR CNRS 6554, Nantes, France.

7 ² Université de Bordeaux, UMR 5805, EPOC, Pessac, France.

8 ³ Université de Nantes, France, CRHIA, EA 1163.

9
10 * Corresponding author. E-mail: maanan-m@univ-nantes.fr

11 **Abstract**

12 This paper details a high-resolution record of French Atlantic coast extreme wave events
13 using a multi-proxy analysis of dated sedimentary deposits. Two lagoons 1) the Petite Mer de
14 Gâvres and 2) the Traicts du Croisic were chosen to identify damaging storm events from the
15 last 300 years with Beeker sampling, ²¹⁰Pb and ¹³⁷Cs dating and sedimentary analysis. Using
16 two new geochemical proxies in the French Atlantic coast, Sr/Fe and Ca/Ti, shows that
17 several storminess events are reported in the nine cores drilled. By correlation with historical
18 archives, seven major storms are confirmed: 1924 AD, 1940 AD, 1972 AD, 1977 AD, 1990
19 AD, 1999 AD, and an 1896 AD highly damaging event. Four other XIXth and XVIIIth century
20 extreme wave event correlations are also proposed from this multi-proxy analysis: 1775 AD,
21 1811 AD, 1838 AD and 1876 AD. Societal and natural impacts caused by these coastal floods
22 are revealed using our dense and varied historical archives.

23
24 **Keywords:** French Atlantic coast, storm events, geochemical ratios, historical archives, 1896
25 event.

26
27 **Highlights**

28 Good sedimentological and historical correlation for the last three centuries

29 Sr/Fe and Ca/Ti are two proxies useful for detecting recent washover in the French Atlantic
30 coast

31 Eleven extreme events recorded in French Atlantic coast sediments

32

33 **1. Introduction**

34 Since the 1990s, there has been a major increase in paleostorm studies, particularly in North
35 America, which is the most studied continent for the geomorphological reconstruction of past
36 storms (Bennington and Farmer, 2014; Boldt et al., 2010; Das et al., 2013; Horwitz and
37 Wang, 2005; Liu and Fearn, 2000, 1993; Mann et al., 2009; Parris et al., 2009). These
38 researches help coastal American societies to better understand the past stormy dynamics of
39 their area. This knowledge is needed to face damaging events and build a more resiliency
40 coastal system as it seems the global coastal population will increase (Chaumillon et al., 2017;
41 Lutz and Samir, 2010; Naylor et al., 2017). By contrast, only a few recent sedimentological
42 paleostorm studies have focused on the French coasts, and most of them concern the
43 Mediterranean coastline. Sabatier et al., 2008 reconstructed three stormy events from the last
44 250 years, while Degeai et al., 2015 attempted to find a storminess periodicity in the last 3000
45 years in the north-western Mediterranean Sea, where the tide amplitude is very low with only
46 a few centimeters. Along the French Atlantic coast, the tidal regime is much higher and cliff
47 top deposits have mainly been used to reconstruct recent historical storm variations (Fichaut
48 and Suanez, 2011; Suanez et al., 2009). From a sedimentological analysis, different types of
49 recent marine deposits on the south-western coastline have been distinguished (Baumann et
50 al., 2017). However, Anthropocene storm analysis is still mainly based on statistics and wave
51 modeling (Bardet et al., 2011; Bertin et al., 2014; Breilh et al., 2013). As several storms have
52 recently hit western French coasts, such as Xynthia in 2010 (Breilh et al., 2014; Regnaud,
53 1999; Regnaud and Kuzucuoglu, 1992; Ruin et al., 2008; Suanez and Cariolet, 2010; Vinet et
54 al., 2012), we focused our study on central western France to detect recent damaging Atlantic
55 storms and analyze their impact by a comparison with historical records.

56 Recent works have proved that grain size is not the only foolproof proxy for extreme wave
57 events (Goto et al., 2012; Szczuciński et al., 2016) as it can be affected by backflow erosion.
58 Thus, geochemistry seems to be a better tool to detect these events (Chagué-Goff et al., 2017).
59 In the absence of previous attempts to define geochemical indicators of past storms for the
60 European Atlantic coast, our objective was to test geochemical proxies testifying to marine
61 conditions in two coastal depositional environments. These proxies will provide a 300-year
62 high-resolution record of extreme wave events from dated sedimentary deposits. Combined
63 with our dense historical resources, these strong events will be associated with the precise
64 date of past storms that impacted the French Atlantic coast, with details about the damage
65 caused by these events.

66 **2. Material and methods**

67 **2.1. Study area**

68 Two study sites were selected based on three criteria : i) back barrier coastal depositional
69 environments; ii) not impacted by man for at least 300 years, with a constant natural
70 evolution; iii) in an area threatened by coastal flooding.

71 Appropriate sites were chosen after a GIS chronological analysis based on IGN (French
72 National Geographic Institute) data. Historical maps were combined with recent aerial
73 photographs to evaluate the evolution of urbanization and the landscape (Pouzet et al., 2015).
74 A topographic analysis was carried out to assess the most relevant back barrier depositional
75 environments. Finally, two of these were selected, directly exposed to coastal flooding on the
76 central western French coast (Le Roy et al., 2015). This comparison revealed that the Traicts
77 du Croisic (central Pays-de-la-Loire region) and the Petite Mer de Gâvres (southern Brittany)
78 lagoons have been well preserved during the last three hundred years. They seem to be
79 appropriate depositional environments for a reconstruction of storminess.

80 The Petite Mer de Gâvres (southern Brittany) and the Traicts du Croisic (central Pays-de-la-
81 Loire) are two coastal marshes with a high morphogenic activity (Fig. 1). These two back
82 barrier lagoons are separated from the sea by a sandy barrier so are useful to detect recent past
83 storms (Baldock et al., 2008; Pierce, 1970; Sabatier et al., 2010; Switzer and Jones, 2008;
84 Zecchetto et al., 1997). They correspond to two different types of lagoon. First, the Petite Mer
85 de Gâvres, near the city of Lorient, is located in a protected natural area. It is a well-formed
86 lagoon, where the barrier beach was already built in the mid-XIXth century (Fig. 1). Based on
87 the sedimentological surface study realized by the Service Hydrographique et
88 Océanographique de la Marine (SHOM) which is available on the database at *data.shom.fr*
89 (*modified*), the Petite Mer de Gâvres can be divided in three distinct sedimentological
90 sections. The western part which is open to the sea is mainly composed of sands, due to its
91 direct tidal connection with the Atlantic Ocean, whereas the eastern back section is more
92 isolated, and shows sediments that are mainly of mostly clayey type. A silty surface offers a
93 slight transition between these two distinct sediment types (Fig. 2A). After a preliminary core
94 test, we chose to sample two different sections of the barrier beach to detect potential
95 differences in the record of storminess between a thin (cores LA1 and LA2) and a thick (cores
96 LB1 and LB2) high protecting dune barrier, in the clayey dominated section (Fig. 1, Fig. 2B).
97 On the other hand, the Traicts du Croisic, situated 100 km west of Nantes, is an open lagoon,
98 which is closing, separated from the sea by a coastal spit that has been growing for centuries:
99 this site corresponds to an actively morphogenic area, also located behind a high protecting
100 dune. The two main channels bring sandy sediments from the ocean by the south-western
101 inlet which rapidly transited by a silty, then clayey type dominating sediment by moving
102 away until the back protected section (Fig. 2A). A longitudinal transect was made of five
103 different cores, behind the thinner part of the barrier and far from the channel's influence,
104 mainly located in a silty soil. Starting from T1 near the dune up to T5 in the center of the
105 marsh, we wanted to recover homogeneous and continuous deposits. A large channel
106 remobilizes sediments in this lagoon, but the first aerial photograph taken in 1948 (from the

107 IGN) shows that it has not moved in the last 70 years (Fig. 1, Fig. 2B). This channel is
108 unlikely to have an impact on the sediment archives.

109 The French Atlantic coast has a semi-diurnal tidal regime; the highest tidal ranges of the two
110 sites are around 6 to 7 meters (according to the SHOM). In our area, waves reach higher
111 heights but shorter periods than in southern France. With main WSW and WNW directions,
112 wintery waves can reach nearly 2.2 meters at l'Ile d'Yeu, located at 50km south from the
113 Traicts du Croisic, whereas they approximately reach 1.45 meters during the summer (Butel
114 et al., 2002). Considering that protecting dunes reach nearly 10 meters NGF (Nivellement
115 General de France, 0 meter NGF is the French topographical reference for the Mean Sea
116 Level, linked to the Mean Sea Level of Marseille, France), only past storms that matched the
117 high tide can be observed. Exposed to extratropical storms that present a mean duration of 4.5
118 days, events mainly come from the ocean during the winter, with a trajectory coming from the
119 SW (Lozano et al., 2004). In the whole Europe, the number and the wind speed of these
120 strong winter events seem to have increased over several decades (Zappa et al., 2013)

121 **2.2. Sampling and sediment analysis**

122 Nine short sediment cores were collected in August 2016 using an Eijkelpkamp© gravity corer,
123 50 mm in diameter and 100 cm in maximum length, to sample into a humid clayey or silty
124 soil. A plastic hammer was used to penetrate the ground, and then a piston avoided
125 compression during the extraction of each humid core. Trimble Differential Global
126 Positioning System (DGPS) was used to survey core positions. All locations were linked to
127 geo-referenced IGN benchmarks and leveled with respect to the NGF datum. Each core was
128 longitudinally sliced and each half-section photographed and described. High-resolution
129 elemental analyses of split sediment cores were carried out using an Avaatech© XRF core
130 scanner. Element intensities normalized by the total intensity (count per second of each
131 spectrum: cps) (Bouchard et al., 2011; Martin et al., 2014), and element ratios (Chagué-Goff,
132 2010; Sabatier et al., 2012) were considered. To complement the sedimentological
133 description, the Scopix© system was used to take X radiographs (Migeon et al., 1998);
134 lightness was estimated by colorimetric analyses (Debret et al., 2011; Polonia et al., 2013)
135 with a Minolta© Cm-2600d spectrometer, as a positive correlation between lightness and
136 carbonate content has already been demonstrated (Mix et al., 1995). The magnetic
137 susceptibility of each centimeter of the nine different cores was measured with an MS2E-1©
138 Bartington-type (Bloemendal and deMenocal, 1989; Wassmer et al., 2010), which has been
139 previously used with success in other studies (Begét et al., 1990; Buynevich et al., 2011; Roy
140 et al., 2010). Then sediment cores were sampled every 0.5 cm for dating, and every 1 cm for
141 grain size, which was measured by a Malvern Mastersizer 2000© laser beam grain sizer
142 (Parsons, 1998; Yu et al., 2009).

143 **2.3. Dating**

144 The age-depth models of cores LB1 and T1 were established from a combination of two
145 short-lived radionuclides. First, ^{210}Pb is a naturally-occurring radionuclide that is incorporated
146 rapidly into the sediment from atmospheric fallout and water column scavenging. This ^{210}Pb ,
147 referred to as ^{210}Pb in excess ($^{210}\text{Pb}_{\text{xs}}$), decays in sediment over time, according to its half-life
148 ($T_{1/2} = 22.3$ years). On the other hand, ^{137}Cs ($T_{1/2} = 30$ years) is an artificial radionuclide,
149 which has well-known pulse inputs related to the atmospheric nuclear weapon tests in the
150 early sixties (maximum atmospheric fallout in 1963 in the northern hemisphere) and, to a
151 lesser extent, to the Chernobyl accident in April 1986.

152 Core descriptions were used to select samples for dating, excluding the sand layers that are
153 not appropriate for ^{210}Pb determination. The activities of ^{210}Pb , ^{226}Ra and ^{137}Cs were
154 determined at the University of Bordeaux on 2.5-4 g of dried sediment by gamma
155 spectrometry, using a well-type, high efficiency low background γ detector equipped with a
156 Cryo-cycle (CANBERRA©). The detector was calibrated using certified reference materials
157 (IAEA-RGU-1; IAEA-IAEA135). Activities are expressed in mBq g⁻¹ and errors based on 1
158 standard-deviation counting statistics. $^{210}\text{Pb}_{\text{xs}}$ was determined by subtracting the activity
159 supported by its parent isotope, ^{226}Ra , from the measured ^{210}Pb activity in the sediment. For
160 the two cores investigated in this work, sediment accumulation rates were calculated from the
161 sedimentary profiles of $^{210}\text{Pb}_{\text{xs}}$, plotted against depth. The deposition time (in years) of the
162 sediment layer was obtained by dividing the depth per unit area by SAR. The deposition year
163 for each sediment layer was subsequently estimated based on the 2016 sampling date for the
164 sediment-water interface.

165 **2.4. Historical archives**

166 As explained above in the introduction, extreme storms recently hit the western French coast.
167 These hazards highlighted the need for an efficient historical reconstruction through the
168 analysis of past storms and marine submersion over the last centuries. Unlike the Netherlands
169 (Gottschalk, 1977, 1975, 1971) or Britain (Bailey, 1991; Hickey, 1997; Lamb and
170 Frydendahl, 1991), research on the history of storms in France is very recent, mostly dating
171 from the past 7 years (Chaumillon et al., 2014; Noël, 2014; Péret and Sauzeau, 2014;
172 Sarrazin, 2012). Although the historical method can be helpful in the sedimentary approach
173 and the study of past storms and sea floods, multidisciplinary approaches, like the one
174 proposed in this paper, are not very widespread and often integrate the historical data rather
175 superficially (Breilh et al., 2014; Van Vliet Lanoe et al., 2014).

176 The historical research is mainly based on ancient documents: i) ancient maps, ii) narrative
177 sources (chronicles, diaries, memories etc.) and iii) documents (books of accounts, records of
178 repairs, surveys conducted after a disaster, barometric observations, newspapers etc.)
179 preserved in libraries and in municipal, departmental, and national archives. These documents
180 contain observational and descriptive data on past extreme weather hazards (descriptions of

181 the storm and the damage caused), as well as impacts on societies and their reactions and
182 adaptation. For the period studied in this paper, we also considered instrumental data such as
183 barometric information and data from Meteo France. In order to cover and reconstruct the
184 history of storms and sea flooding that occurred on the central western French coast over the
185 last 300 years, we consulted more than 398 documents, of which only 264 contained data on
186 past storms and coastal floods.

187 Before being used to reconstruct the history of storms and sea flooding over a relatively long
188 period, these data had to be studied, analyzed, criticized and included in databases to produce
189 cross-checking. To consider a written document (and its data) reliable, details about the
190 writing of the document, i.e. who was the author, if he/she witnessed (or not) the event, what
191 was the institutional framework and so on, had to be defined (Athimon and Maanan, 2018).
192 Moreover, when possible, it was necessary to cross-check the hazard testimonies with several
193 sources. The aim was to have a more precise and exhaustive view of the event in order to
194 characterize it, spot potential errors more easily and reconstruct the history of storms within a
195 defined temporal and spatial frame. Like any method, there are some limitations of the
196 historical reconstruction of storms and sea floods (Athimon and Maanan, 2018): the most
197 important is probably the loss of countless documents and data, especially during the French
198 Revolution and wars like the Second World War. However, this does not prevent the
199 historical climatologist from identifying and characterizing important storms and sea floods of
200 the past.

201 **2.5. Statistical analysis**

202 Multivariate statistical analysis was used to investigate the geochemical structure (continental
203 or marine context data) of the sediments quantitatively, and to extract the geochemical
204 markers characterizing an extreme event of marine origin. Calculations were performed on
205 606 sediment samples, 357 from the Traicts du Croisic and 249 from La Petite Mer de
206 Gâvres, using statistical analysis according to the recommendation of van Hattum et al., 1991.
207 Based on the Pearson correlation coefficient, each potential stormy proxy was correlated to
208 each other. A Principal Component Analysis has been made using R© software to sort these
209 elements into two groups (Yamasoe et al., 2000), testifying to two different types of deposit
210 origin: lagoonal and allochthonous (marine) elements. The sorting have been automatically
211 made by the software after a dendrogram summarization of the ACP, using libraries “*vegan*”
212 and “*cluster*” of the software. The most opposed elements were then used to test geochemical
213 ratios that could potentially testify to oceanic conditions. These ratios helped to determine the
214 stormy layers specific to the French Atlantic coast, in these two specific environments.

215 **3. Results and discussion**

216 **3.1. Dating and age-depth modeling**

217 At the Traicts du Croisic (TC), the lower parts of the five cores are mostly composed by sand.
218 The upper layers consist mainly of silty clay, but a gradual decrease in its thickness, from 30
219 cm in core T1 to nearly 10 cm in core T3, is noticeable with the distance from the coastline
220 (Fig. 2C). Cores T4 and T5, both extracted the furthest from the high protecting dune, show a
221 high composition of sands, with a thin 5-cm silt horizon in the upper layers and an increasing
222 sand grain size downcore. There are no earthworms or air holes, which mean that bioturbation
223 can be excluded in all Croisic cores.

224 In the Petite Mer de Gâvres (PMG), the cores extracted at two different locations present two
225 different stratigraphic profiles (Fig. 2C). In the LB area, the top of each core starts with fine-
226 grained sediment, mainly composed of clay or silt. Deeper, from about 35 to 50 cm (LB1) or
227 20 to 60 (LB2), there is a coarser-grained layer, which presents a high variability in grain size
228 (fine sand to a 6-cm diameter pebble) testifying to a difference in sediment origin. The base of
229 the PMG-LB cores again presents fine-grained sediment. In PMG-LA cores, there is a
230 sandy/silt main variation after a thin 10-cm fine-grained sediment top layer. The end of these
231 two cores (last five centimeters) is also finer than the dominant sands. In the same way as in
232 the Traicts du Croisic marsh, no bioturbation marker is observed in all four PMG cores.

233 Based on the core description, we selected one core per site for dating. At the Traicts du
234 Croisic, core T1 presents the thickest clayey top layer (nearly 30 cm) and appears the most
235 appropriate for radionuclide determinations. In the Petite Mer de Gâvres (PMG), LB1 is the
236 finest-grained core with an intermediate layer between 35 and 50 cm consisting of coarse sand
237 and pebbles. This layer was considered a hydrodynamic event and was not sampled for
238 radionuclide determination.

239 The profile of $^{210}\text{Pb}_{\text{xs}}$ with depth in core T1 is rather classic, with activities decreasing
240 exponentially to reach negligible levels below 20 cm (Fig. 3, A). A mean sediment
241 accumulation rate of 0.24 cm yr^{-1} was estimated. The ^{210}Pb chronology indicates that core T1
242 ranges from 1916 ± 13 to 2016. This estimate is supported by the sedimentary ^{137}Cs profile;
243 ^{137}Cs activities disappear rapidly to negligible levels below a deep peak at about 12-13 cm,
244 which corresponds to 1963 according to the ^{210}Pb dating.

245 In the Petite Mer de Gâvres (PMG), core LB1 presents lower activities of radionuclides,
246 which could be related to a higher sedimentation rate and coarser sediments (Fig. 3, B).
247 $^{210}\text{Pb}_{\text{xs}}$ presents the same decreasing trend with depth in the sediment as already observed for
248 core T1. In addition, low levels of $^{210}\text{Pb}_{\text{xs}}$ were measured below the sand layer. Mean
249 sedimentation accumulation rates are about 0.37 cm yr^{-1} . The ^{210}Pb chronology indicates that
250 the base of the sand layer is about 1896 ± 10 . Although at low levels, the ^{137}Cs profile
251 supports this chronology.

252 For horizons beyond the timescale covered by ^{210}Pb , we extrapolated the ages by assuming
253 that the mean sedimentation rate determined for each site, 0.4 cm yr^{-1} (PMG) and 0.2 cm yr^{-1} ,
254 (TC) was constant.

255 **3.2. Cored sediments characteristics**

256 *3.2.1. Development of extreme event indicators*

257 A statistical correlation analysis was carried out to sort the correlated elements into two
258 different groups, testifying to two distinct types of sediment: continental and allochthonous.
259 Part of the American massif, the watershed is an association of “two mica” leucogranites:
260 magnesium peraluminic and alkali granites rich in potassium (Capdevila, 2010). Continental
261 major layers will thus present high proportions of metal elements. Our statistical results show
262 a high opposition of two elements, Ca and Sr, (also well correlated to each other with a
263 correlation coefficient cc. of 0.96, Table 1) with all other elements including those found in
264 the watershed (Fig.4, Fig.5). Si is the only exception isolated alone as it can be found in both
265 continental and marine sediments. Thus, three groups can be observed with analysis of the
266 correlation coefficient and the automatized sorting function of the dendrogram : i)
267 allochthonous and marine elements: Ca and Sr; ii) continental elements, and particularly
268 lacustrine, for this study site: Br, Cl, Co, Cu, Fe, K, Pb, Rb, Ti and Zn (cc. around 0.5 and
269 more), and secondarily Al, K, Ni, and Zr (cc. between 0.2 and 0.5); iii) Si, which can be found
270 in both environments. Finally, Mn and S are the two only elements with no correlation with
271 another. PCA shows that Mn can be regrouped with marine elements, whereas S is closer than
272 the continental group. Ca and Sr can provide a good extreme wave event signature from
273 marine carbonate, where high radioactivity can be found into shells debris (Bozzano et al.,
274 2002; Chagué-Goff et al., 2017; Degeai et al., 2015; Raji et al., 2015; Sabatier et al., 2010;
275 Szczuciński et al., 2005). Strontium is also used into some paleotsunami studies, proving that
276 it could be a significant proxy of sea saltwater sediment incomes (Cuven et al., 2013; Nichol
277 et al., 2007). As these two seem to be very distinct from the other elements, and particularly
278 those corresponding to the watershed, we tested Ca/Ti and Sr/Fe ratios for the first time in the
279 European Atlantic coastline.

280 *3.2.2. Traicts du Croisic*

281 All five cores show two different systems with a base of coarser grain sized, and generally
282 more marine geochemical elements (Fig. 6). The 20-30 cm upper part of the cores shows
283 lower morphogenic activity, with mostly silt or clayey sediment and lower Sr/Fe, Ca/Ti and
284 lightness with higher MS values, testifying to more continental inputs. This large difference
285 between these two systems is due to the evolution of the sandy spit, which became thicker
286 with time (Fig. 1, Fig. 6), thus isolating this north-western part of the coastal marsh from the
287 sea. This is why more storminess is identified in the coarser base of the core than in the upper

288 clayey layer: as the spit became thicker during the last decade, the upstream marsh became
289 more protected from the sea. Storms cannot disturb this environment now as much as when
290 the dune was thinner.

291 All five cores show correlations of proxies increase between grain size, Sr/Fe and Ca/Ti
292 ratios, lightness and a decrease in magnetic susceptibility. The tenth decile is also used as a
293 new stormy proxy here. As it represents only 10 percent of the finest fraction of each sample,
294 a high D10 shows overall coarse sediment (at least for 90 percent of its composition). T1
295 shows this clear multiple correlation near cm. 35 (coarse sandy layer with increase in Sr/Fe
296 and Ca/Ti from 0 to 0.3 and 0 to 3), with a peak in lightness (45 to 50%) and a fall in MS (10
297 to 8 SI) indicating an allochthonous marine layer. As erosion can affect storm markers, we
298 also report the large increase in the two geochemical ratios at cm. 61 in this core, even though
299 the grain size stays constant. These two storm markers are also seen in the T2 core, which
300 testifies to the most impacted area because five other marine allochthonous layers are
301 observed. Three of them are very noticeable at cms. 40, 35 and 30 with a high grain size and
302 geochemistry peaks. The last two are slighter storminess events observed at cms. 17 and 10.
303 T3 presents four probable storminess events observed at cms. 17, 29, 43 and 61 with high
304 proxy variations, testifying to huge differences with the surrounding finer grained layers. T4
305 and T5 are similar with two marine layers observed at cms. 31 and 17 but with two last
306 marine intrusion observed only in the T4 core at cms. 7 and 59, and one last in the T5 core at
307 cm. 5 (Fig. 6).

308 3.2.3. *Petite Mer de Gâvres*

309 In the Petite Mer de Gâvres, the well-formed basin studied has been closed and isolated from
310 the sea for centuries. Therefore, only a unique sedimentological profile can be detected here,
311 in contrast to the Traicts du Croisic sedimentological analysis (Fig. 7). This profile is defined
312 by fine grain sized sediments (silt or clay), with low Sr/Fe, Ca/Ti, lightness with a high MS
313 for an area affected by the continent and well isolated from the sea. In the same way as in the
314 Croisic analysis, storminess can be detected by coarser grain sized sediments coming from
315 marine washovers, with an increase in these two geochemical ratios and lightness, and a
316 possible decrease in MS.

317 Two different sites were drilled, "LA" and "LB", because our preliminary core tests showed
318 that an important storminess variation is recorded behind a thick (LB) and a thin (LA) dune
319 barrier (Fig. 1, Fig. 7). First, an important storminess is recorded near cm. 50 in the LB area,
320 with coarse pebbles detected between two clayey layers. A 6-cm diameter pebble was
321 extracted from the core. These pebbles come from the mixed sandy/pebbly beach on the other
322 side of the dune barrier (photograph I, Fig. 7), confirming the washover origin of this layer.
323 Furthermore, the nearshore sediment surface is also composed by pebbles, thus demonstrating
324 their marine origin (Fig. 2A). In our core analyses, no pebble is observed in the LA

325 environment although we think that it was impacted as much as LB, as shown by the
326 sedimentology comparisons and dating carried out in these two sites. In the LA area, we can
327 assume that this significant event breached the dune barrier where the vegetation is less dense,
328 and that the wave backflow evacuated these coarser deposits. Geochemical ratios show that
329 storminess is also recorded in the LA area, without these pebbles. In the LB environment, it is
330 the opposite: the thicker sandy barrier caught the pebbles in the marsh, explaining why they
331 were found during drilling. According to sediment observations and analysis results, this
332 storminess corresponds to the marine input at 45-50 cm depth of the LA area. The fall in the
333 Ca/Ti ratio is due to measurement disturbances made by a hole where a marine shell was
334 removed before analysis, and with its correlation with the low MS values and increase of
335 lightness and Sr/Fe ratio, proves the marine input for this section.

336 Moreover, with the method previously described, other significant allochthonous layers are
337 reported: sedimentological analyses show another marine intrusion at cm. 35 for LA1; at cms.
338 10, 15, 25 and 35 for LA2; at cms. 5 and 35 for LB1; and at cms. 5, 15, 25 and 35 for LB2
339 (Fig. 7).

340 **3.3. Historic records of extreme events**

341 *3.3.1. Coupling with historical data*

342 Our searches found 149 storms, including twenty sea floods, recorded in historical documents
343 from the middle of the XVIIIth century to today. From historical archives, eleven marine
344 floods correlating with stormy conditions have been recorded in the XXth century, six in the
345 XIXth century, and three in the second part of the XVIIIth century. Into these twenty events,
346 fourteen of them reports damage in the two study areas, whereas the six others only impacted
347 the Croisic study area (Pays-de-la-Loire region) and didn't damaged the Gâvres site (Brittany
348 region). Since the middle of the XVIIIth century, storms appear much more extreme in the
349 Northern Atlantic (Hickey, 1997; Lamb and Frydendahl, 1991), and from the second part of
350 the 19th century, they seem more numerous (Desarthe, 2013). However, it is necessary to be
351 careful: historical documentation is more available for the XVIIIth - XXth centuries than for
352 earlier periods. Moreover, the development of modern meteorology since the second part of
353 the XIXth century and the use of relatively recent technology such as satellite views may
354 distort researchers' observations and interpretations.

355 *3.3.2. Extreme event reconstruction*

356 From the sedimentological analysis, periods attesting to allochthonous layers coming into
357 these two clayey lagoons were extracted. By correlation with the historical archives, we found
358 a precise extreme wave event date for each of these layers reported. No notable tsunami has
359 been identified in the historical records for the last 200 years in our area (Dawson et al., 2004;

360 Karnik, 1971), so we assume that these marine layers come mainly from stormy conditions.
361 The French Atlantic coast experiences high tidal ranges; we conclude that stormy events have
362 to combine with high tides to disturb these natural environments. Consequently, marine layers
363 observed in these cores are overwashes due to stormy events combined with high tide
364 conditions. As ^{137}Cs and ^{210}Pb activities stop near 1890 AD, we kept only XXth century dates
365 as high certainty events. For the earlier ones assessed by extrapolation of the sedimentation
366 rate, we allowed only the estimated geological periods as a result. From the sedimentology,
367 we extracted seven main storminess post 1896 dates and four high probable earliest
368 hypothesis. The historical archives enabled us to have a more precise dating. We know that all
369 the events were from Atlantic depressions, with mostly southerly or southwesterly high
370 winds, and some with known high tide coefficients. They also provide clues about the
371 environmental and societal destruction, to assess the real impact of these extreme wave
372 events.

373 Overall, results demonstrate a good correlation between historical archives and
374 sedimentological results. From the twenty marine flooding dates recorded into historical data,
375 eleven have been identified in our nine sedimentological cores. The nine others that have not
376 been identified are explained by a sedimentological storm record limit, and by the precision of
377 historical data and their damage location details. First, we cannot record successive storms in
378 sediment archives. With a mean sedimentation rate of 0.25cm/yr, a centimeter depth of a core
379 does correspond to a four year sedimentation period. If successive marine flooding occurs in
380 less than a five-years period, only one marine layer can be recorded (Chaumillon et al., 2017;
381 Liu and Fearn, 1993; Pouzet et al., 2018). This can be the case for the 1987 AD and 1990 AD
382 events in the study site. Moreover, an important historical limit cannot allow the building of a
383 complete correlation. Some past storms, as the very devastating 1760 AD event, recorded a
384 high marine flooding at Bouin, just 50 kilometers south from the Traicts du Croisic
385 (Departmental Archives of Vendée: 8 B 32). This event has been taken into account in the
386 database as a destructive event for the Croisic area, as damages were identified near the study
387 site. However, we cannot be sure that this marine flooding also occurs in our cored area, since
388 the very old reference that mention this storm, while being precise, does not necessarily report
389 all the damages made everywhere by this storm. From our sedimentological results, the non-
390 presence of marine input in the Croisic cores confirms that it may not have impacted the area
391 as well as the Bouin site. If the coupling of historical and sedimentological archives allows us
392 to confirm sedimentological results, the sedimentology can also increase the flawed
393 knowledge of some past storms.

394 The great majority of storms are not violent enough to affect societies and ecosystems
395 dramatically. Since only the most extreme events are recorded in sediments, once these data
396 are coupled with historical observations, meteorological characteristics and descriptions of the
397 damage caused, we can refine the knowledge of some important hazards. This makes the
398 combination of different methods introduced in this paper relevant, because as the coastal

399 population is expected to increase during the next decades (Lutz and Samir, 2010), the
400 damages enhanced by coastal flooding will undoubtedly follow these dynamics (Chaumillon
401 et al., 2017). With a better knowledge on past stormy dynamics, coastal societies directly
402 exposed to this hazard will be prepared to face it, and consequently be less vulnerable to their
403 induced damages. Past storm historical chronologies are essential to assess extreme events
404 recurrence intervals and to subsequently prepare society more reliably to face the future storm
405 and coastal flooding hazards (Goslin and Clemmensen, 2017). Therefore, for their wide
406 source of historical information, palaeodata have to be included in risk assessment to better
407 prepare coastal societies and enable them to develop a more resilient way of life (Naylor et
408 al., 2017).

409 i) Traicts du Croisic cores

410 T1, located just behind the sandy barrier, only records a pre-XXth century storm. Its location
411 too near the sandy barrier probably prevented later overwash deposits (Fig. 1, Fig. 6). Just two
412 overwashes are recorded there, when the coastal split was thinner. From T2 to T5, numerous
413 marine flooding markers are recorded, with a growing signature gradient from the barrier to
414 the center of the lagoon: the core located nearest the coastline records the most storminess,
415 while the three others have only four potential markers. With the five cores retained, four
416 main certain and accurate dates for the XXth century can be determined from our historical
417 research: 26th February 1990 (cm. 5 for T4 core), 11th January 1978 (cm. 7 for T5 core), 13th
418 February 1972 (cm. 10 for T2 and T5 cores) and 17th November 1940 (cm. 15-20 for T2, T3,
419 T4 and T5 cores). From historical records, three different storms crossed the study area in
420 1990, including its strongest that crossed a 104 high tide coefficient (SHOM) on February 26-
421 28, 1990. The three storms caused 100 fatalities over the whole country, with winds reaching
422 176 km/h maximum in western France and many reports of flooded houses and broken dikes
423 (<http://tempetes.meteofrance.fr/Daria-le-25-janvier-1990.html>, <http://tempetes.meteofrance.fr/Herta-le-03-fevrier-1990.html>,
424 <http://tempetes.meteofrance.fr/Viviane-du-26-au-28-fevrier-1990.html>;
425 Municipal Archives of Nantes, 23 Z 355; 24 PRES 152, 05/02/1990 and 24 PRES
426 152, 27 and 28/02/1990, Departmental Archives of Vendée, 1856 W 38). The second date
427 from found in sedimentology is 1977. From historical archives, the two different events of
428 December 2, 1976 or January 11, 1978 can be related. As in the first case the tide coefficient
429 was very low, ca. only 50, and it reached 109 in the second (SHOM), the second date is
430 therefore more likely. With ten deaths and fatalities reported, the 1978 storm crossed a large
431 part of the country with damage notified from Dunkerque to the Gironde estuary (numerous
432 shipwrecks and marine flooding reported in Le Marin 1595, MetMar 101 and (Steers et al.,
433 1979) for other English damages). Historical records show that these two last earlier storms of
434 1972 and 1940 created a wind speed of 200 km/h that uprooted trees, damaged bell towers,
435 toppled cranes, destroyed dikes, boats and roofs with many coastal floods. While the second
436 one mostly hit western France (<http://tempetes.meteofrance.fr/Tempete-du-13-fevrier-1972.html>;
437 Municipal Archives of Nantes, 1038 W 327; Departmental Archives of Vendée,

438 78/31 1953-1975 – tempête du 13 février 1972), the first affected the whole country for three
439 days, destroying whole forests and leading to nearly 30 deaths
440 (<http://tempetes.meteofrance.fr/Tempete-du-16-au-17-novembre-1940.html>); Departmental
441 Archives of Loire-Atlantique, 75 W 274 –31/12/1940, 75 W 274 – 18/02/1941, 75 W 274 –
442 12/05/1941; Departmental Archives of Vendée, BIB B 1036/1-2).

443 Four other extreme wave events are recorded with sedimentation rate extrapolation at around
444 1890 AD (cm. 30-35 for all five cores), 1880-75 AD (cm. 35 for T2), 1840-35 AD (cm. 40-45
445 for T2 and T3), 1810-1800 AD (cm. 50 for T2), and around 1775-1770 AD (cm. 55-60 for T1,
446 T2, T3 and T4). From historical records matches, they correspond to the high impacting
447 storms of 31st December 1876 – 1st January 1877 AD, creating nearly 25 kilometers of
448 breaches into the Croisic dikes, with three millions Francs (more than 500 000 \$) total
449 damage estimated (Departmental Archives, 575 S 1, 7 S 181, Journal L'Union Bretonne –
450 11/01/1877 (numerisation)); to the 24th/25th February 1838 AD event, creating “*considerable*
451 *damages*” according to the former home secretary (Journal de la Charente Inférieure,
452 01/03/1838-04/04/1838; Municipal Archives of Nantes, 7 PRES 15 – 25/02/1838; (Brunet,
453 1994) Bibliothèque Mazarine, 8° 94560-1 and 8° 94560-2, p. 552); to the 26th February 1811
454 AD storm that totally flooded the island of Bouin, located at 50 kilometers south from the
455 Croisic area (Municipal Archives of Nantes, 55PRES21 03/03/1811; Tardy P., 2000); and to
456 the October 1775 AD intense storm, with a report mentioning that “*the sea goes over the*
457 *roads, overturns and drives a bridge*” (Debresme, 1922). The last 1900-1895 AD marker,
458 impacting all the area, is mentioned in the following section about Petite Mer de Gâvres.

459 There are various consequences of the Croisic extreme events recorded in the historical
460 documents, according to the intensity and recurrence of the hazard. Damages are mostly
461 human, economic, and material. The event of January 1877 is well documented. An extreme
462 storm hit the west of France, in particular the studied area. Strong west-south-west winds
463 coupled with a strong tidal coefficient generated a phenomenon of overtide. Breaking with
464 power, the sea crashed onto the land causing significant damage: 25 kilometers of dykes at
465 Croisic were completely destroyed, the salt marshes of Guerande were submerged by the sea,
466 public health was compromised by stagnant water, the loss of salt production was estimated at
467 between 25 and 50% and the amount of money to repair the infrastructure was exorbitant
468 (Departmental Archives, 575 S 1, 7 S 181, Journal L'Union Bretonne – 11/01/1877).

469 ii) Petite Mer de Gâvres cores

470 The combination of proxies revealed three main dates observed for Croisic of 1990 (cm. 10 of
471 LA2), 1972 (cm. 15-20 for LB2 and LA2) and 1940 (cm. 25-30 for LB2 and LA2) (Fig. 7).
472 As they disturbed two different lagoons 100 km apart, these three storms deeply impacted a
473 large part of the French Atlantic coast. Moreover, two main other storminess events are seen
474 in several Gâvres cores. Using historical archives, these were precisely dated to 9th January

475 1924, and 26th/27th December 1999. These two different dates testify to two destructive
476 storms. In 1924 (storminess observed at cm. 30-35 in all four cores), a 100 km/h wind speed
477 combined with a 100 tidal coefficient event hit all the Atlantic coasts and drowned ten people
478 (Météo France: <http://tempetes.meteofrance.fr/Tempete-du-8-au-9-janvier-1924.html>; Journal
479 Ouest Éclair, 10/01/1924; Journal La Vendée Républicaine, 12/01/1924; Journal L'Etoile de la
480 Vendée, 13/01/1924; Municipal Archives of Nantes, 304 PRES 838; Departmental Archives
481 of Loire-Atlantique, 109 S 167, 05/11/1927). In 1999 (cm. 5 in LB), all the country was hit
482 and nearly a hundred dead were reported during these two series of storms reaching 200 km/h
483 wind speeds (<http://tempetes.meteofrance.fr/Martin-les-27-et-28-decembre-1999.html>; 24
484 PRES 270, 30/12/1999; 24 PRES 271, 06/01/2000).

485 The last important marker was dated circa 1895–1900, which brought the 6-cm diameter
486 pebble into the LB environment (Fig. 7). As a clayey layer was dated underneath the pebble
487 horizon, our dating estimates the overwash near 1896. In addition, our dating on top of this
488 layer is estimated at near 1915, so it would have taken nearly twenty years to re-stabilize the
489 environment after this highly damaging event. From historical archives, we know that the
490 storm hit the whole country on 4th December 1896, and that numerous breaches were
491 reported, which makes the Gâvres breach hypothesis very likely. This information was
492 extracted from a dozen sources, including a visual testimony. A tsunami might have brought
493 this pebble layer, but the region is rarely hit by this kind of hazard (Dawson et al., 2004;
494 Karnik, 1971). Furthermore, this date does not correspond to any tsunami record in the
495 archives, which is why we favor the powerful storm hypothesis. This event caused 33 deaths
496 in France during flooding created by the storm that combined with a high tide coefficient of
497 95 according to the SHOM (Météo-France: <http://tempetes.meteofrance.fr/Tempete-du-4-decembre-1896.html>; Journal de la Charente Inférieure, 09/12/1896; Departmental Archives
498 of Loire-Atlantique, 575 S 1; 7 R 1/1509; 3 Z 195; Departmental Archives of Vendée, 1 M
499 558). We propose the hypothesis that this damaging event affected a large part of the French
500 Atlantic coast as a Croisic hypothesis is set at around 1890 (Fig. 6). Markers found in the
501 Gâvres cores may correspond to this Croisic hypothesis, reported in all nine cores of this
502 study. As the upper contact with the clayey layer is dated around 1915 AD, we estimated the
503 resilience of the Gâvres lagoon system to be nearly twenty years after this high impacting
504 event.
505

506 **4. Conclusion**

507 Coupling historical and sedimentological archives helps to date recent marine deposits and
508 obtain information about extreme wave events. We detected three main impacting storm dates
509 found in the two different sites: 1990 AD, 1972 AD and 1940 AD. Three other stormy events
510 also disturbed one of the two lagoons: 1924 AD, 1977 AD and 1999 AD, with four other 19th
511 and XVIIIth century extreme wave event hypotheses reported in the central western French

512 coast: 1775 AD, 1811 AD, 1838 AD and 1876 AD. Moreover, we propose that an important
513 storm event completely disturbed a part of the French Atlantic coast in 1896 AD.

514 Based on statistical analyses, we also tested two new geochemical ratios never previously
515 used in the French Atlantic coast: Sr/Fe and Ca/Ti. Coupling these ratios with other
516 sedimentological analyses showed their usefulness in detecting recent storms. Historical
517 archives proved that these storm hypotheses agree with sedimentological storminess dates,
518 particularly due to these two new geochemical ratios. Further work must now be done to
519 extend this European Atlantic storm analysis earlier to confirm pre-XXth century dates with
520 the large historical French archive collection available.

521 **5. Acknowledgments**

522 The authors gratefully acknowledge Isabelle Billy and her sedimentary core technical team of
523 the EPOC (University of Bordeaux 1) for XRF spectrometric core scanner analysis, and
524 Cassandra Carnet for English corrections. This work was supported by grants from the
525 Fondation de France through the research program « Quels littoraux pour demain? ».

526 **6. References**

- 527 Athimon, E., Maanan, M., 2018. Severe storm, coastal flood damage, adaptation and resilience of
528 societies during the Little Ice Age (West of France). *Prog. Hum. Geogr.* Submitt.
- 529 Bailey, M., 1991. Per impetum maris: natural disaster and economic decline in eastern England,
530 1275-1350, in: *Before the Black Death. Studies in the "crisis" of the Early Fourteenth Century.*
531 Campbell, Manchester-New York, pp. 184–208.
- 532 Baldock, T.E., Weir, F., Hughes, M.G., 2008. Morphodynamic evolution of a coastal lagoon entrance
533 during swash overwash. *Geomorphology* 95, 398–411.
534 <https://doi.org/10.1016/j.geomorph.2007.07.001>
- 535 Bardet, L., Duluc, C.-M., Rebour, V., L'Her, J., 2011. Regional frequency analysis of extreme storm
536 surges along the French coast. *Nat Hazards Earth Syst Sci* 11, 1627–1639.
537 <https://doi.org/10.5194/nhess-11-1627-2011>
- 538 Baumann, J., Chaumillon, E., Schneider, J.-L., Jorissen, F., Sauriau, P.-G., Richard, P., Bonnin, J.,
539 Schmidt, S., 2017. Contrasting sediment records of marine submersion events related to
540 wave exposure, Southwest France. *Sediment. Geol.* 353, 158–170.
541 <https://doi.org/10.1016/j.sedgeo.2017.03.009>
- 542 Begét, J.E., Stone, D.B., Hawkins, D.B., 1990. Paleoclimatic forcing of magnetic susceptibility
543 variations in Alaskan loess during the late Quaternary. *Geology* 18, 40–43.
544 [https://doi.org/10.1130/0091-7613\(1990\)018<0040:PFOMSV>2.3.CO;2](https://doi.org/10.1130/0091-7613(1990)018<0040:PFOMSV>2.3.CO;2)
- 545 Bennington, J.B., Farmer, E.C., 2014. Recognizing Past Storm Events in Sediment Cores Based on
546 Comparison to Recent Overwash Sediments Deposited by Superstorm Sandy, in: *Learning*
547 *from the Impacts of Superstorm Sandy.* Academic Press, pp. 89–106.
- 548 Bertin, X., Li, K., Roland, A., Zhang, Y.J., Breilh, J.F., Chaumillon, E., 2014. A modeling-based analysis of
549 the flooding associated with Xynthia, central Bay of Biscay. *Coast. Eng.* 94, 80–89.
550 <https://doi.org/10.1016/j.coastaleng.2014.08.013>
- 551 Bloemendal, J., deMenocal, P., 1989. Evidence for a change in the periodicity of tropical climate
552 cycles at 2.4 Myr from whole-core magnetic susceptibility measurements. *Nature* 342, 897–
553 900. <https://doi.org/10.1038/342897a0>

554 Boldt, K.V., Lane, P., Woodruff, J.D., Donnelly, J.P., 2010. Calibrating a sedimentary record of
555 overwash from Southeastern New England using modeled historic hurricane surges. *Mar.*
556 *Geol.* 275, 127–139. <https://doi.org/10.1016/j.margeo.2010.05.002>

557 Bouchard, F., Francus, P., Pienitz, R., Laurion, I., 2011. Sedimentology and geochemistry of
558 thermokarst ponds in discontinuous permafrost, subarctic Quebec, Canada. *J. Geophys. Res.*
559 *Biogeosciences* 116, G00M04. <https://doi.org/10.1029/2011JG001675>

560 Bozzano, G., Kuhlmann, H., Alonso, B., 2002. Storminess control over African dust input to the
561 Moroccan Atlantic margin (NW Africa) at the time of maxima boreal summer insolation: a
562 record of the last 220 kyr. *Palaeogeogr. Palaeoclimatol. Palaeoecol.* 183, 155–168.
563 [https://doi.org/10.1016/S0031-0182\(01\)00466-7](https://doi.org/10.1016/S0031-0182(01)00466-7)

564 Breilh, J.-F., Bertin, X., Chaumillon, É., Giloy, N., Sauzeau, T., 2014. How frequent is storm-induced
565 flooding in the central part of the Bay of Biscay? *Glob. Planet. Change* 122, 161–175.
566 <https://doi.org/10.1016/j.gloplacha.2014.08.013>

567 Breilh, J.F., Chaumillon, E., Bertin, X., Gravelle, M., 2013. Assessment of static flood modeling
568 techniques: application to contrasting marshes flooded during Xynthia (western France). *Nat*
569 *Hazards Earth Syst Sci* 13, 1595–1612. <https://doi.org/10.5194/nhess-13-1595-2013>

570 Brunet, R., 1994. *Ars, notre beau village: chronique d'une commune de l'île de Ré au cours de deux*
571 *siècles d'histoire.* R. Brunet, La Rochelle.

572 Butel, R., Dupuis, H., Bonneton, P., 2002. Spatial variability of wave conditions on the French Atlantic
573 coast using in-situ data. *J. Coast. Res.* 36, 96–108.

574 Buynevich, I., Klein, A., FitzGerald, D., Cleary, W., Hein, C., Veiga, F., Angulo, R., Asp, N., Petermann,
575 R., 2011. Geological legacy of storm erosion along a high-energy indented coastline: northern
576 Santa Catarina, Brazil. *J. Coast. Res.* 1840–1844.

577 Capdevila, R., 2010. Les granites varisques du Massif Armoricain. *Bull. Société Géologique*
578 *Minéralogique Bretagne Série D*, 1–52.

579 Chagué-Goff, C., 2010. Chemical signatures of palaeotsunamis: A forgotten proxy? *Mar. Geol.* 271,
580 67–71. <https://doi.org/10.1016/j.margeo.2010.01.010>

581 Chagué-Goff, C., Szczuciński, W., Shinozaki, T., 2017. Applications of geochemistry in tsunami
582 research: A review. *Earth-Sci. Rev.* 165, 203–244.
583 <https://doi.org/10.1016/j.earscirev.2016.12.003>

584 Chaumillon, E., Bertin, X., Fortunato, A.B., Bajo, M., Schneider, J.-L., Dezileau, L., Walsh, J.P.,
585 Michelot, A., Chauveau, E., Créach, A., Hénaff, A., Sauzeau, T., Waeles, B., Gervais, B., Jan, G.,
586 Baumann, J., Breilh, J.-F., Pedreros, R., 2017. Storm-induced marine flooding: Lessons from a
587 multidisciplinary approach. *Earth-Sci. Rev.* 165, 151–184.
588 <https://doi.org/10.1016/j.earscirev.2016.12.005>

589 Chaumillon, E., Garnier, E., Sauzeau, T., 2014. *Les Littoraux à l'heure du changement climatique.* Les
590 Indes savantes, Paris.

591 Cuyen, S., Paris, R., Falvard, S., Miot-Noirault, E., Benbakkar, M., Schneider, J.-L., Billy, I., 2013. High-
592 resolution analysis of a tsunami deposit: Case-study from the 1755 Lisbon tsunami in
593 southwestern Spain. *Mar. Geol.* 337, 98–111. <https://doi.org/10.1016/j.margeo.2013.02.002>

594 Das, O., Wang, Y., Donoghue, J., Xu, X., Coor, J., Elsner, J., Xu, Y., 2013. Reconstruction of paleostorms
595 and paleoenvironment using geochemical proxies archived in the sediments of two coastal
596 lakes in northwest Florida. *Quat. Sci. Rev.* 68, 142–153.
597 <https://doi.org/10.1016/j.quascirev.2013.02.014>

598 Dawson, A.G., Lockett, P., Shi, S., 2004. Tsunami hazards in Europe. *Environ. Int.* 30, 577–585.
599 <https://doi.org/10.1016/j.envint.2003.10.005>

600 Debret, M., Sebag, D., Desmet, M., Balsam, W., Copard, Y., Mourier, B., Susperrigui, A.-S., Arnaud, F.,
601 Bentaleb, I., Chapron, E., Lallier-Vergès, E., Winiarski, T., 2011. Spectrocolorimetric
602 interpretation of sedimentary dynamics: The new “Q7/4 diagram.” *Earth-Sci. Rev.* 109, 1–19.
603 <https://doi.org/10.1016/j.earscirev.2011.07.002>

604 Degeai, J.-P., Devillers, B., Dezileau, L., Oueslati, H., Bony, G., 2015. Major storm periods and climate
605 forcing in the Western Mediterranean during the Late Holocene. *Quat. Sci. Rev.* 129, 37–56.
606 <https://doi.org/10.1016/j.quascirev.2015.10.009>

607 Desarthe, J., 2013. *Le temps des saisons - Climat, événements extrêmes et sociétés dans l’Ouest de la*
608 *France (XVIe-XIXe siècles)*. Paris : Hermann éditeurs des sciences et des arts.

609 Fichaut, B., Suanez, S.S., 2011. Quarrying, transport and deposition of cliff-top storm deposits during
610 extreme events: Banneg Island, Brittany. *Mar. Geol.* 283, 36–55.
611 <https://doi.org/10.1016/j.margeo.2010.11.003>

612 Goslin, J., Clemmensen, L.B., 2017. Proxy records of Holocene storm events in coastal barrier
613 systems: Storm-wave induced markers. *Quat. Sci. Rev.* 174, 80–119.
614 <https://doi.org/10.1016/j.quascirev.2017.08.026>

615 Goto, K., Chagué-Goff, C., Goff, J., Jaffe, B., 2012. The future of tsunami research following the 2011
616 Tohoku-oki event. *Sediment. Geol., The 2011 Tohoku-oki tsunami* 282, 1–13.
617 <https://doi.org/10.1016/j.sedgeo.2012.08.003>

618 Gottschalk, M.K.E., 1977. *Stormvloeden en rivieroverstromingen in Nederland, vol.3*. Van Gorcum &
619 Comp, Assen/Amsterdam.

620 Gottschalk, M.K.E., 1975. *Stormvloeden en rivieroverstromingen in Nederland, vol.2*. Van Gorcum &
621 Comp, Assen/Amsterdam.

622 Gottschalk, M.K.E., 1971. *Stormvloeden en rivieroverstromingen in Nederland, vol.1*. Van Gorcum &
623 Comp, Assen/Amsterdam.

624 Hickey, K.R., 1997. *Documentary records of coastal storms in Scotland, 1500- 1991 A.D.* PhD Thesis
625 602.

626 Horwitz, M.H., Wang, P., 2005. Sedimentological Characteristics and Internal Architecture of Two
627 Overwash Fans From Hurricanes Ivan and Jeanne. *Géology Fac. Publ.*

628 Karnik, V., 1971. *Seismicity of the European Area*. Springer.

629 Lamb, H., Frydendahl, K., 1991. *Historic Storms of the North Sea, British Isles and Northwest Europe*.
630 Cambridge University Press.

631 Le Roy, S., Pedreros, R., André, C., Paris, F., Lecacheux, S., Marche, F., Vinchon, C., 2015. Coastal
632 flooding of urban areas by overtopping: dynamic modelling application to the Johanna storm
633 (2008) in Gâvres (France). *Nat Hazards Earth Syst Sci* 15, 2497–2510.
634 <https://doi.org/10.5194/nhess-15-2497-2015>

635 Liu, K., Fearn, M.L., 2000. Reconstruction of Prehistoric Landfall Frequencies of Catastrophic
636 Hurricanes in Northwestern Florida from Lake Sediment Records. *Quat. Res.* 54, 238–245.
637 <https://doi.org/10.1006/qres.2000.2166>

638 Liu, K., Fearn, M.L., 1993. Lake-sediment record of late Holocene hurricane activities from coastal
639 Alabama. *Geology* 21, 793–796. [https://doi.org/10.1130/0091-](https://doi.org/10.1130/0091-7613(1993)021<0793:LSROLH>2.3.CO;2)
640 [7613\(1993\)021<0793:LSROLH>2.3.CO;2](https://doi.org/10.1130/0091-7613(1993)021<0793:LSROLH>2.3.CO;2)

641 Lozano, I., Devoy, R.J.N., May, W., Andersen, U., 2004. Storminess and vulnerability along the Atlantic
642 coastlines of Europe: analysis of storm records and of a greenhouse gases induced climate
643 scenario. *Mar. Geol., Storms and their significance in coastal morpho-sedimentary dynamics*
644 210, 205–225. <https://doi.org/10.1016/j.margeo.2004.05.026>

645 Lutz, W., Samir, K., 2010. Dimensions of global population projections: what do we know about
646 future population trends and structures? *Philos. Trans. R. Soc. Lond. B Biol. Sci.* 365, 2779–
647 2791. <https://doi.org/10.1098/rstb.2010.0133>

648 Mann, M.E., Woodruff, J.D., Donnelly, J.P., Zhang, Z., 2009. Atlantic hurricanes and climate over the
649 past 1,500 years. *Nature* 460, 880–883. <https://doi.org/10.1038/nature08219>

650 Martin, L., Mooney, S., Goff, J., 2014. Coastal wetlands reveal a non-synchronous island response to
651 sea-level change and a palaeostorm record from 5.5 kyr to present. *The Holocene* 24, 569–
652 580. <https://doi.org/10.1177/0959683614522306>

653 Migeon, S., Weber, O., Faugeres, J.-C., Saint-Paul, J., 1998. SCOPIX: A new X-ray imaging system for
654 core analysis. *Geo-Mar. Lett.* 18, 251–255. <https://doi.org/10.1007/s003670050076>

655 Mix, A.C., Harris, S.E., Janecek, T.R., 1995. Estimating lithology from nonintrusive reflectance spectra :
656 Leg 138.

657 Naylor, L.A., Spencer, T., Lane, S.N., Darby, S.E., Magilligan, F.J., Macklin, M.G., Möller, I., 2017.
658 Stormy geomorphology: geomorphic contributions in an age of climate extremes. *Earth Surf.*
659 *Process. Landf.* 42, 166–190. <https://doi.org/10.1002/esp.4062>

660 Nichol, S.L., Goff, J.R., Devoy, R.J.N., Chagué-Goff, C., Hayward, B., James, I., 2007. Lagoon subsidence
661 and tsunami on the West Coast of New Zealand. *Sediment. Geol., Sedimentary Features of*
662 *Tsunami Deposits - Their Origin, Recognition and Discrimination: An Introduction* 200, 248–
663 262. <https://doi.org/10.1016/j.sedgeo.2007.01.019>

664 Noël, S., 2014. La vulnérabilité des populations de la côte Est du Cotentin 1700-1914 : l'approche
665 historique dans l'analyse des enjeux, de l'aléa et de la gestion du risque de submersion, in:
666 Actes Du Colloque International, Connaissance et Compréhension Des Risques Côtiers. IUEM
667 de Brest, p. 445–455.

668 Parris, A.S., Bierman, P.R., Noren, A.J., Prins, M.A., Lini, A., 2009. Holocene paleostorms identified by
669 particle size signatures in lake sediments from the northeastern United States. *J. Paleolimnol.*
670 43, 29–49. <https://doi.org/10.1007/s10933-009-9311-1>

671 Parsons, M.L., 1998. Salt Marsh Sedimentary Record of the Landfall of Hurricane Andrew on the
672 Louisiana Coast: Diatoms and Other Paleoindicators. *J. Coast. Res.* 14, 939–950.
673 <https://doi.org/10.2307/4298846>

674 Péret, J., Sauzeau, T., 2014. Xynthia ou la mémoire réveillée. Des villages charentais et vendéens face
675 à l'océan (XVIIIe-XXIe siècles), Geste. ed. La Crèche.

676 Pierce, J.W., 1970. Tidal Inlets and Washover Fans. *J. Geol.* 78, 230–234.
677 <https://doi.org/10.1086/627504>

678 Polonia, A., Bonatti, E., Camerlenghi, A., Lucchi, R.G., Panieri, G., Gasperini, L., 2013. Mediterranean
679 megaturbidite triggered by the AD 365 Crete earthquake and tsunami. *Sci. Rep.* 3, 1285.
680 <https://doi.org/10.1038/srep01285>

681 Pouzet, P., Creach, A., Godet, L., 2015. Dynamique de la démographie et du bâti dans l'ouest du
682 Marais poitevin depuis 1705. *Norois Environ. Aménage. Société* 83–96.
683 <https://doi.org/10.4000/norois.5589>

684 Pouzet, P., Maanan, M., Piotrowska, N., Baltzer, A., Stéphan, P., Robin, M., 2018. Chronology of
685 Holocene storm events along the European Atlantic coast : new data from the Island of Yeu,
686 France. *Prog. Phys. Geogr.*

687 Raji, O., Dezileau, L., Von Grafenstein, U., Niazi, S., Snoussi, M., Martinez, P., 2015. Extreme sea
688 events during the last millennium in the northeast of Morocco. *Nat Hazards Earth Syst Sci* 15,
689 203–211. <https://doi.org/10.5194/nhess-15-203-2015>

690 Regnaud, H., 1999. L'élévation et les variations du niveau marin à l'Holocène terminal dans l'Ouest
691 français : une approche par les dépôts de tempêtes [Sea-level elevation and variation during
692 late holocene in western France ; storm surge relicts as indicators]. *Quaternaire* 10, 181–188.
693 <https://doi.org/10.3406/quate.1999.1641>

694 Regnaud, H., Kuzucuoglu, C., 1992. Rebuilding of a dune field landscape after a catastrophic storm :
695 beaches of Ille et Vilaine, Brittany, France, in: Carter R.W.G., S.-S.M.J., Curtis T.G.S. (Ed.),
696 Coastal Dunes, Geomorphology, Ecology and Management for Conservation. Balkema, pp.
697 379–387.

698 Roy, P.D., Caballero, M., Lozano, R., Ortega, B., Lozano, S., Pi, T., Israde, I., Morton, O., 2010.
699 Geochemical record of Late Quaternary paleoclimate from lacustrine sediments of paleo-lake
700 San Felipe, western Sonora Desert, Mexico. *J. South Am. Earth Sci.* 29, 586–596.
701 <https://doi.org/10.1016/j.jsames.2009.11.009>

702 Ruin, I., Creutin, J.-D., Anquetin, S., Lutoff, C., 2008. Human exposure to flash floods – Relation
703 between flood parameters and human vulnerability during a storm of September 2002 in
704 Southern France. *J. Hydrol.* 361, 199–213. <https://doi.org/10.1016/j.jhydrol.2008.07.044>

705 Sabatier, P., Dezileau, L., Briquieu, L., Colin, C., Siani, G., 2010. Paleostorm events revealed by clay
706 minerals and geochemistry in coastal lagoon: a study case of Pierre Blanche (NW
707 Mediterranean Sea). *Sediment. Geol.* 228, 205–217.

708 Sabatier, P., Dezileau, L., Colin, C., Briquieu, L., Bouchette, F., Martinez, P., Siani, G., Raynal, O., Von
709 Grafenstein, U., 2012. 7000 years of paleostorm activity in the NW Mediterranean Sea in
710 response to Holocene climate events. *Quat. Res.* 77, 1–11.
711 <https://doi.org/10.1016/j.yqres.2011.09.002>

712 Sabatier, P., Dezileau, L., Condomines, M., Briquieu, L., Colin, C., Bouchette, F., Le Duff, M.,
713 Blanchemanche, P., 2008. Reconstruction of paleostorm events in a coastal lagoon (Hérault,
714 South of France). *Mar. Geol.* 251, 224–232. <https://doi.org/10.1016/j.margeo.2008.03.001>

715 Sarrazin, J.-L., 2012. « Vimers de mer » et sociétés littorales entre Loire et Gironde (XIVe-XVIe siècle).
716 *Norais* n° 222, 91–102.

717 Steers, J.A., Stoddart, D.R., Bayliss-Smith, T.P., Spencer, T., Durbidge, P.M., 1979. The Storm Surge of
718 11 January 1978 on the East Coast of England. *Geogr. J.* 145, 192–205.
719 <https://doi.org/10.2307/634386>

720 Suanez, S., Cariolet, J.-M., 2010. L'action des tempêtes sur l'érosion des dunes : les enseignements de
721 la tempête du 10 mars 2008. *Norais Environ. Aménagement. Société* 77–99.
722 <https://doi.org/10.4000/norais.3212>

723 Suanez, S., Fichaut, B., Magne, R., 2009. Cliff-top storm deposits on Banneg Island, Brittany, France:
724 Effects of giant waves in the Eastern Atlantic Ocean. *Sediment. Geol.* 220, 12–28.
725 <https://doi.org/10.1016/j.sedgeo.2009.06.004>

726 Switzer, A.D., Jones, B.G., 2008. Large-scale washover sedimentation in a freshwater lagoon from the
727 southeast Australian coast: sea-level change, tsunami or exceptionally large storm? *The*
728 *Holocene* 18, 787–803. <https://doi.org/10.1177/0959683608089214>

729 Szczuciński, W., Niedzielski, P., Rachlewicz, G., Sobczyński, T., Ziola, A., Kowalski, A., Lorenc, S.,
730 Siepak, J., 2005. Contamination of tsunami sediments in a coastal zone inundated by the 26
731 December 2004 tsunami in Thailand. *Environ. Geol.* 49, 321–331.
732 <https://doi.org/10.1007/s00254-005-0094-z>

733 Szczuciński, W., Pawłowska, J., Lejzerowicz, F., Nishimura, Y., Kokociński, M., Majewski, W.,
734 Nakamura, Y., Pawłowski, J., 2016. Ancient sedimentary DNA reveals past tsunami deposits.
735 *Mar. Geol.* 381, 29–33. <https://doi.org/10.1016/j.margeo.2016.08.006>

736 van Hattum, B., Timmermans, K.R., Govers, H.A., 1991. Abiotic and biotic factors influencing in situ
737 trace metal levels in macroinvertebrates in freshwater ecosystems. *Environ. Toxicol. Chem.*
738 10, 275–292. <https://doi.org/10.1002/etc.5620100217>

739 Van Vliet Lanoe, B., Pénaud, A., Hénaff, A., Delacourt, C., Fernane, A., Goslin, J., Hallégouet, B., Le
740 Cornec, E., 2014. Middle- to late-Holocene storminess in Brittany (NW France): Part II - The
741 chronology of events and climate forcing. *Holocene* 24, 434–453.
742 <https://doi.org/10.1177/0959683613519688>

743 Vinet, F., Defossez, S., Rey, T., Boissier, L., 2012. Le processus de production du risque « submersion
744 marine » en zone littorale : l'exemple des territoires « Xynthia ». *Norais* 11–26.

745 Wassmer, P., Schneider, J.-L., Fonfrège, A.-V., Lavigne, F., Paris, R., Gomez, C., 2010. Use of
746 anisotropy of magnetic susceptibility (AMS) in the study of tsunami deposits: Application to
747 the 2004 deposits on the eastern coast of Banda Aceh, North Sumatra, Indonesia. *Mar. Geol.*
748 275, 255–272. <https://doi.org/10.1016/j.margeo.2010.06.007>

749 Yamasoe, M.A., Artaxo, P., Miguel, A.H., Allen, A.G., 2000. Chemical composition of aerosol particles
750 from direct emissions of vegetation fires in the Amazon Basin: water-soluble species and
751 trace elements. *Atmos. Environ.* 34, 1641–1653. [https://doi.org/10.1016/S1352-2310\(99\)00329-5](https://doi.org/10.1016/S1352-2310(99)00329-5)

752
753 Yu, K.-F., Zhao, J.-X., Shi, Q., Meng, Q.-S., 2009. Reconstruction of storm/tsunami records over the
754 last 4000 years using transported coral blocks and lagoon sediments in the southern South
755 China Sea. *Quat. Int.* 195, 128–137. <https://doi.org/10.1016/j.quaint.2008.05.004>

- 756 Zappa, G., Shaffrey, L.C., Hodges, K.I., Sansom, P.G., Stephenson, D.B., 2013. A Multimodel
757 Assessment of Future Projections of North Atlantic and European Extratropical Cyclones in
758 the CMIP5 Climate Models. *J. Clim.* 26, 5846–5862. [https://doi.org/10.1175/JCLI-D-12-](https://doi.org/10.1175/JCLI-D-12-00573.1)
759 00573.1
- 760 Zecchetto, S., Umgiesser, G., Brocchini, M., 1997. Hindcast of a storm surge induced by local real
761 wind fields in the Venice Lagoon. *Cont. Shelf Res.* 17, 1513–1538.
762 [https://doi.org/10.1016/S0278-4343\(97\)00023-X](https://doi.org/10.1016/S0278-4343(97)00023-X)

763

764 Primary Sources of historical archives:

765 - Météo France :

766 <http://tempetes.meteofrance.fr/Tempete-du-4-decembre-1896.html>

767 <http://tempetes.meteofrance.fr/Tempete-du-8-au-9-janvier-1924.html>

768 <http://tempetes.meteofrance.fr/Tempete-du-16-au-17-novembre-1940.html>

769 <http://tempetes.meteofrance.fr/Tempete-du-13-fevrier-1972.html>

770 <http://tempetes.meteofrance.fr/Daria-le-25-janvier-1990.html>

771 <http://tempetes.meteofrance.fr/Herta-le-03-fevrier-1990.html>

772 <http://tempetes.meteofrance.fr/Viviane-du-26-au-28-fevrier-1990.html>

773 <http://tempetes.meteofrance.fr/Martin-les-27-et-28-decembre-1999.html>

774 - Municipal Archives of Nantes :

775 1038 W 327

776 55PRES21, 03/03/1811

777 23 Z 355

778 7 PRES 15 – 25/02/1838

779 24 PRES 152, 05/02/1990, Presse Océan

780 24 PRES 152, 27-28/02/1990, Presse Océan

781 24 PRES 270, 30/12/1999, Presse Océan

- 782 24 PRES 271, 06/01/2000, Presse Océan
- 783 304 PRES 838, 12/01/2014, Presse Océan
- 784 - Departmental Archives of Loire-Atlantique :
- 785 7 S 181
- 786 7 R 1/1509
- 787 109 S 167, 05/11/1927
- 788 575 S 1
- 789 75 W 274, 31/12/1940
- 790 75 W 274, 18/02/1941
- 791 75 W 274, 12/05/1941
- 792 3 Z 195
- 793 - Departmental archives of Vendée :
- 794 1 M 558
- 795 1856 W 38
- 796 78/31 1953-1975 – tempête du 13 février 1972
- 797 BIB B 1036/1-2
- 798 8 B 32
- 799 - Others :
- 800 Journal de la Charente Inférieure, 01/03/1838 – 04/04/1838
- 801 Journal L'Union Bretonne – 11/01/1877 (numerisation)
- 802 Journal de la Charente inférieure, 09/12/1896
- 803 Journal Ouest-Eclair, 10/01/1924

- 804 Journal La Vendée républicaine, 12/01/1924, n°2073
- 805 Journal L'Etoile de la Vendée, 13/01/1924, n°4359
- 806 Le Marin 20 Janvier 1978 N°1595
- 807 MetMar 1978 N°101
- 808 Athimon E., Maanan M., Sauzeau T., Sarrazin J-L., 2016, « Vulnérabilité et adaptation des
809 sociétés littorales aux aléas météo-marins entre Guérande et l'île de Ré, France (XIVe -
810 XVIIIe siècle) », *Vertigo*, 16-3, [online].
- 811 Bailey, M., 1991, "Per impetum maris: natural disaster and economic decline in eastern
812 England, 1275-1350", in : Campbell (ed.), *Before the Black Death. Studies in the "crisis" of*
813 *the early fourteenth century*, Manchester-New York, pp. 184-208.
- 814 Debresme M., « Journal de Marc Debresme (1700-1784) », in *Bulletin et Mémoires de la*
815 *Société archéologique et historique de Charente*, t. XIII, 1922, p. 79-126.
- 816 Ministère de la culture et de la communication, 2011, « Archives », Chiffres clés – statistiques
817 de la culture, PDF online :
- 818 https://francearchives.fr/file/0d31b1371ab1324afb6b5dd3e835fc11092a6890/static_5099.pdf
- 819 Hickey K.R., 1997, *Documentary records of coastal storms in Scotland, 1500-1991 A.D.*, 2
820 volumes, Thesis, Coventry University, Coventry.
- 821 Tardy P., 2000, "Cahiers de la mémoire, revue d'art & tradition populaires d'archéologie et
822 d'histoire", n°75
- 823

Table 1. Geochemical correlation matrix

	Al	Br	Ca	Cl	Co	Cu	Fe	K	Mn	Ni	Pb	Rb	S	Si	Sr	Ti	Zn	Zr	
Al	1.00	0.44	-0.12	0.01	0.28	0.29	0.50	0.85	-0.03	0.17	0.46	0.64	0.06	0.25	-0.11	0.57	0.43	0.35	Al
Br		1.00	-0.20	0.55	0.69	0.54	0.83	0.49	0.02	0.26	0.58	0.58	0.33	-0.35	-0.15	0.75	0.76	0.29	Br
Ca			1.00	-0.27	-0.09	-0.11	-0.15	-0.28	0.12	-0.03	-0.18	-0.46	0.31	-0.06	0.96	-0.18	-0.10	-0.22	Ca
Cl				1.00	0.70	0.38	0.70	0.36	-0.05	0.19	0.37	0.45	0.54	-0.82	-0.28	0.66	0.73	0.42	Cl
Co					1.00	0.51	0.86	0.45	0.08	0.19	0.43	0.48	0.59	-0.57	-0.07	0.81	0.83	0.50	Co
Cu						1.00	0.57	0.34	0.05	0.22	0.40	0.37	0.30	-0.26	-0.11	0.53	0.56	0.23	Cu
Fe							1.00	0.63	0.12	0.26	0.60	0.59	0.57	-0.53	-0.13	0.95	0.93	0.46	Fe
K								1.00	-0.13	0.18	0.49	0.84	0.22	-0.03	-0.28	0.69	0.60	0.46	K
Mn									1.00	-0.14	0.04	-0.25	0.12	-0.02	0.10	0.09	0.11	-0.07	Mn
Ni										1.00	0.19	0.15	0.17	-0.12	-0.02	0.26	0.23	0.15	Ni
Pb											1.00	0.51	0.16	-0.16	-0.16	0.56	0.55	0.27	Pb
Rb												1.00	0.07	-0.11	-0.42	0.60	0.57	0.42	Rb
S													1.00	-0.63	0.26	0.55	0.61	0.33	S
Si														1.00	-0.04	-0.46	-0.58	-0.22	Si
Sr															1.00	-0.17	-0.10	-0.22	Sr
Ti																1.00	0.90	0.55	Ti
Zn																	1.00	0.48	Zn
Zr																		1.00	Zr
	Al	Br	Ca	Cl	Co	Cu	Fe	K	Mn	Ni	Pb	Rb	S	Si	Sr	Ti	Zn	Zr	

Figure 1. Historical presentation of the two studied sites

Figure 2. Sedimentological presentation of the two studied sites, with the SHOM sedimentological map (A), the precise core location (B) and the presentation of the nine extracted cores (C)

Figure 3. $^{210}\text{Pb}_{\text{xs}}$ profile with depth and ^{137}Cs profile with age along the cores in the Traicts du Croisic (T1, A) and the Petite Mer de Gâvres (LB1, B)

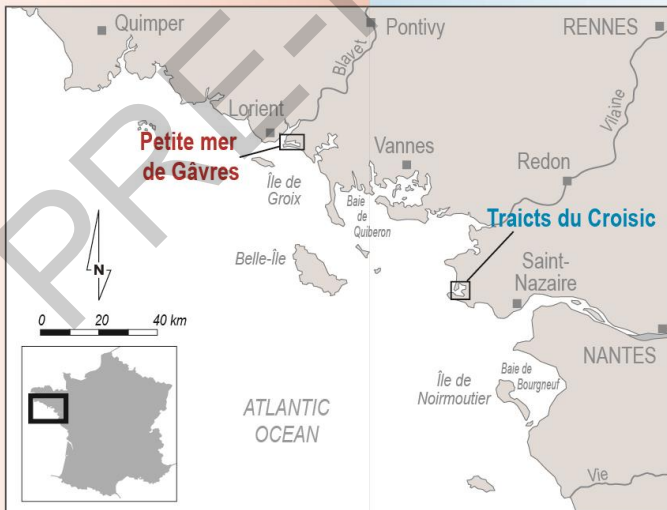
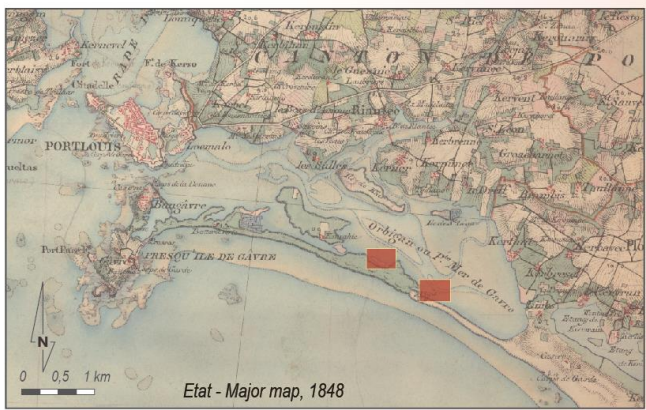
Figure 4. Geochemical elements dendrogram

Figure 5. PCA summarization with automatized group-sorting (blue : marine elements, pink : continental elements, yellow : mixed element)

Figure 6. Detection of Traicts du Croisic paleoevents

Figure 7. Detection of Petite Mer de Gâvres paleoevents

PRE-PRINT

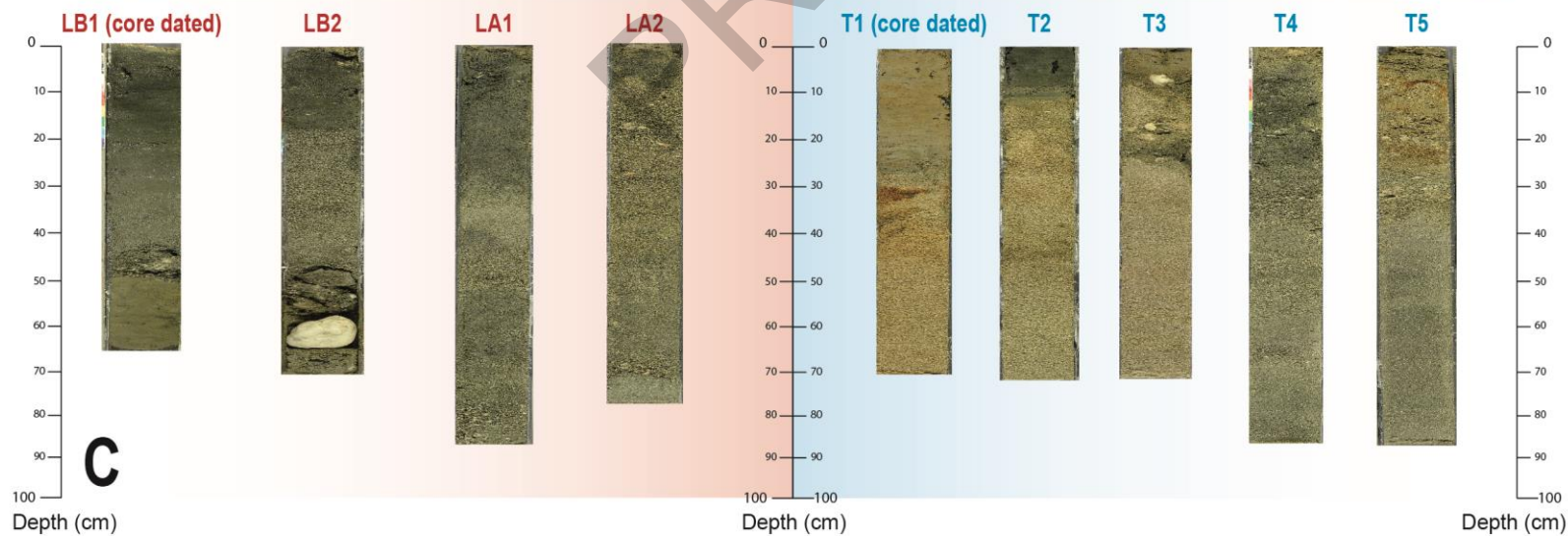
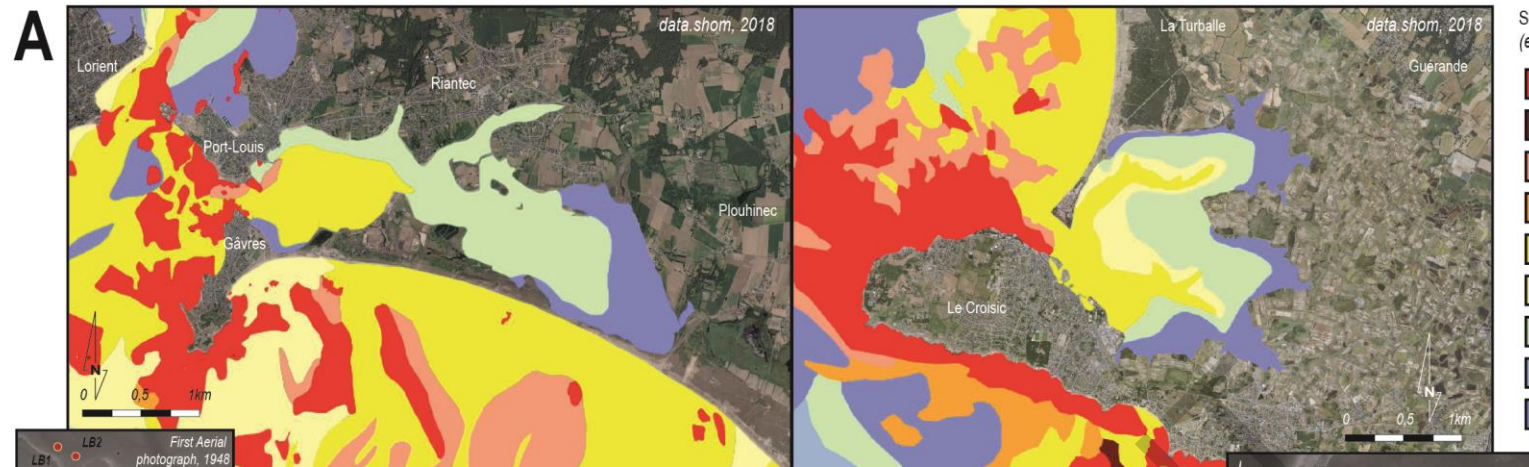


Petite mer de Gâvres

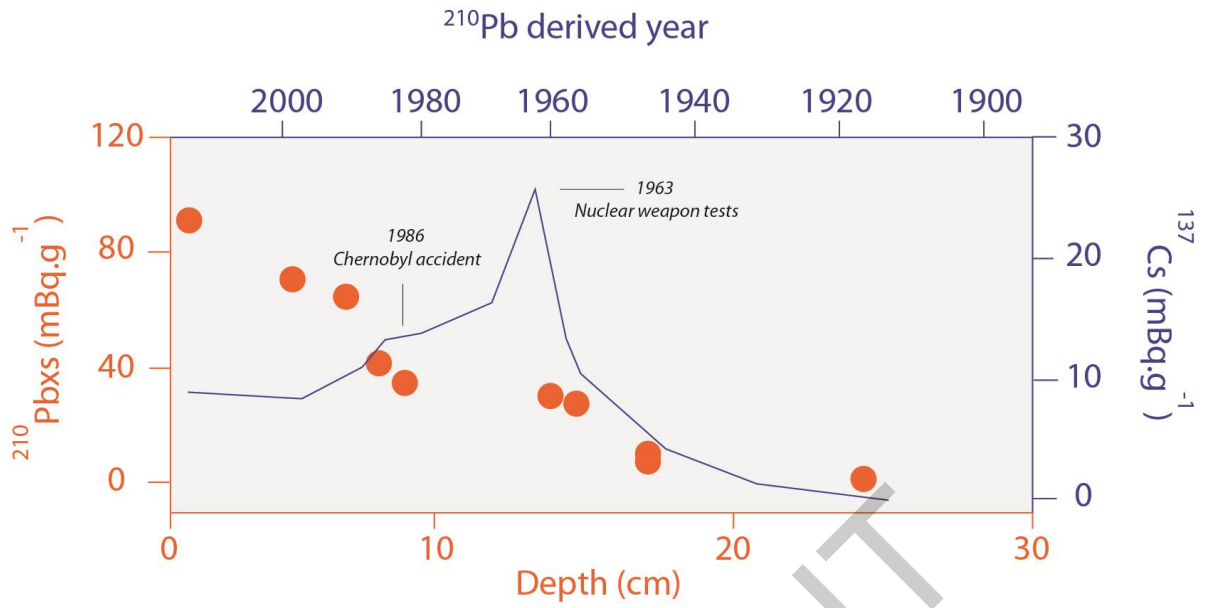
Traits du Croisic

Sedimentological map
(extracted from the SHOM database)

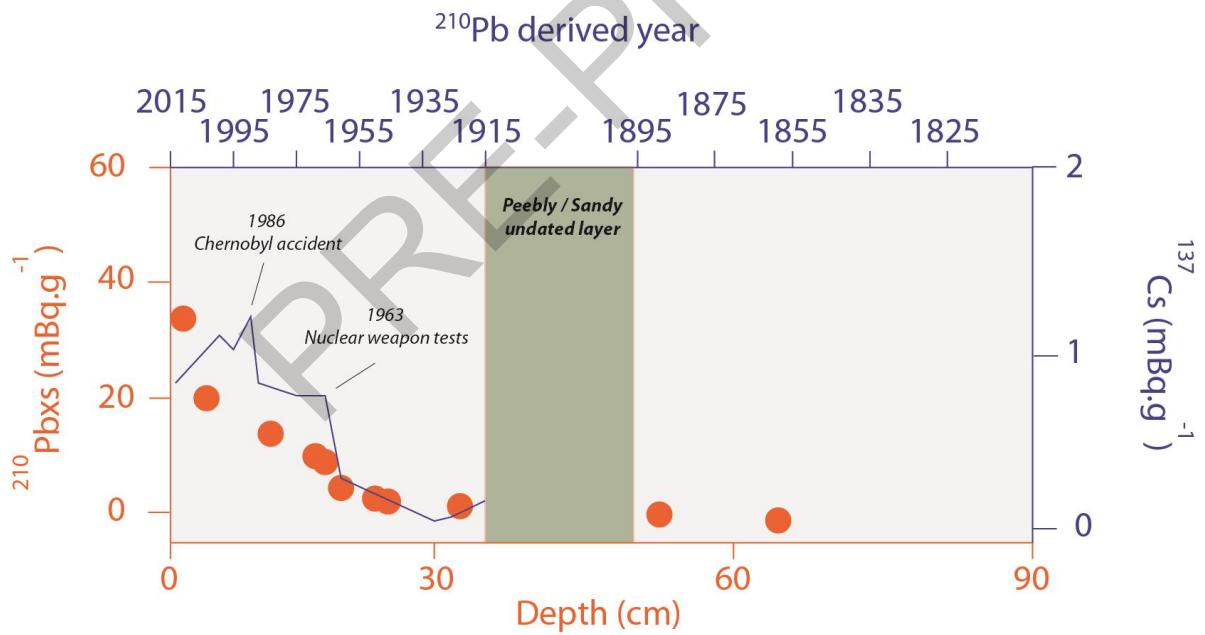
- Rock
- Coarse pebble
- Pebbles
- Coarse sand
- Sand
- Fine sand
- Silt
- Silty clay
- Clay

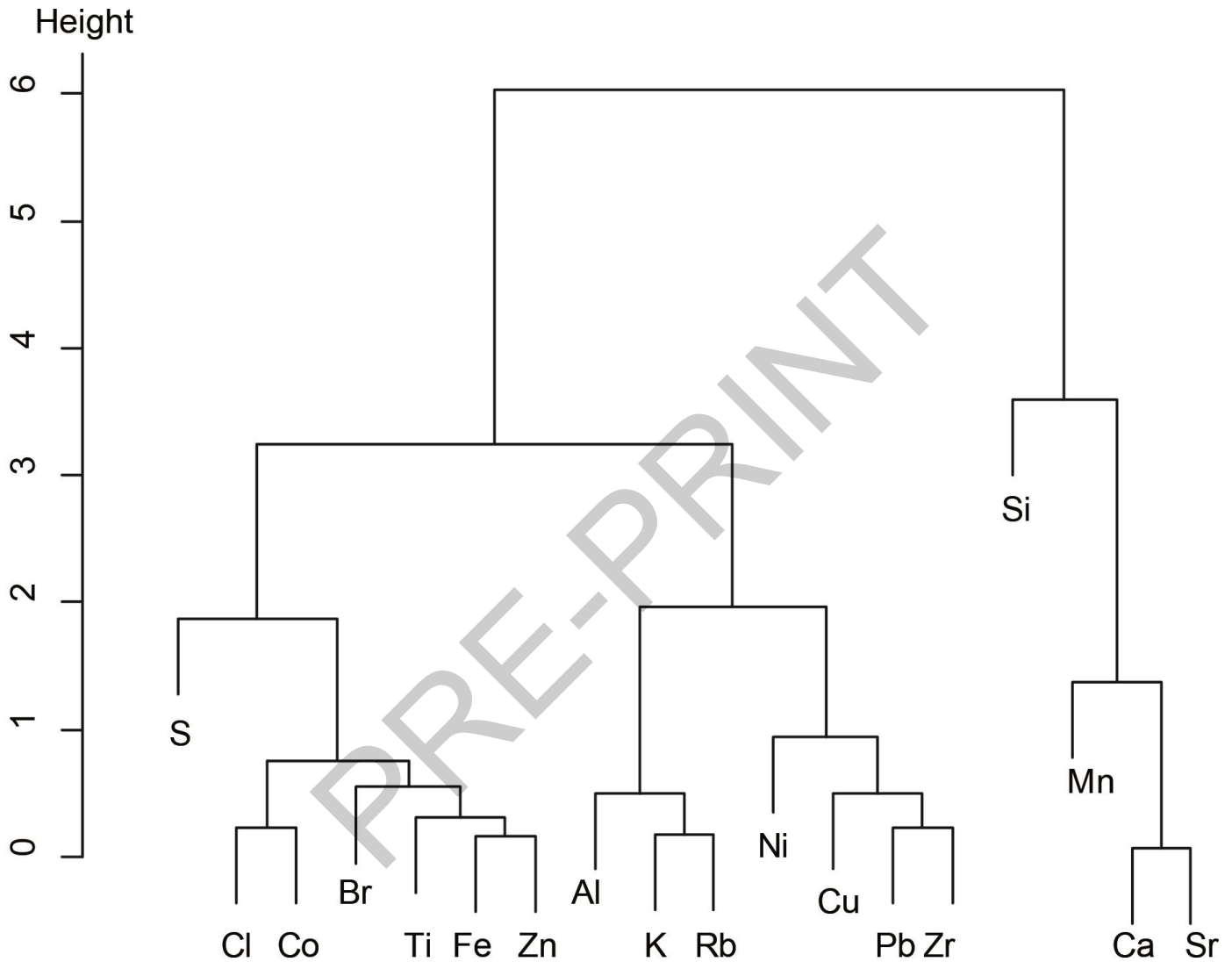


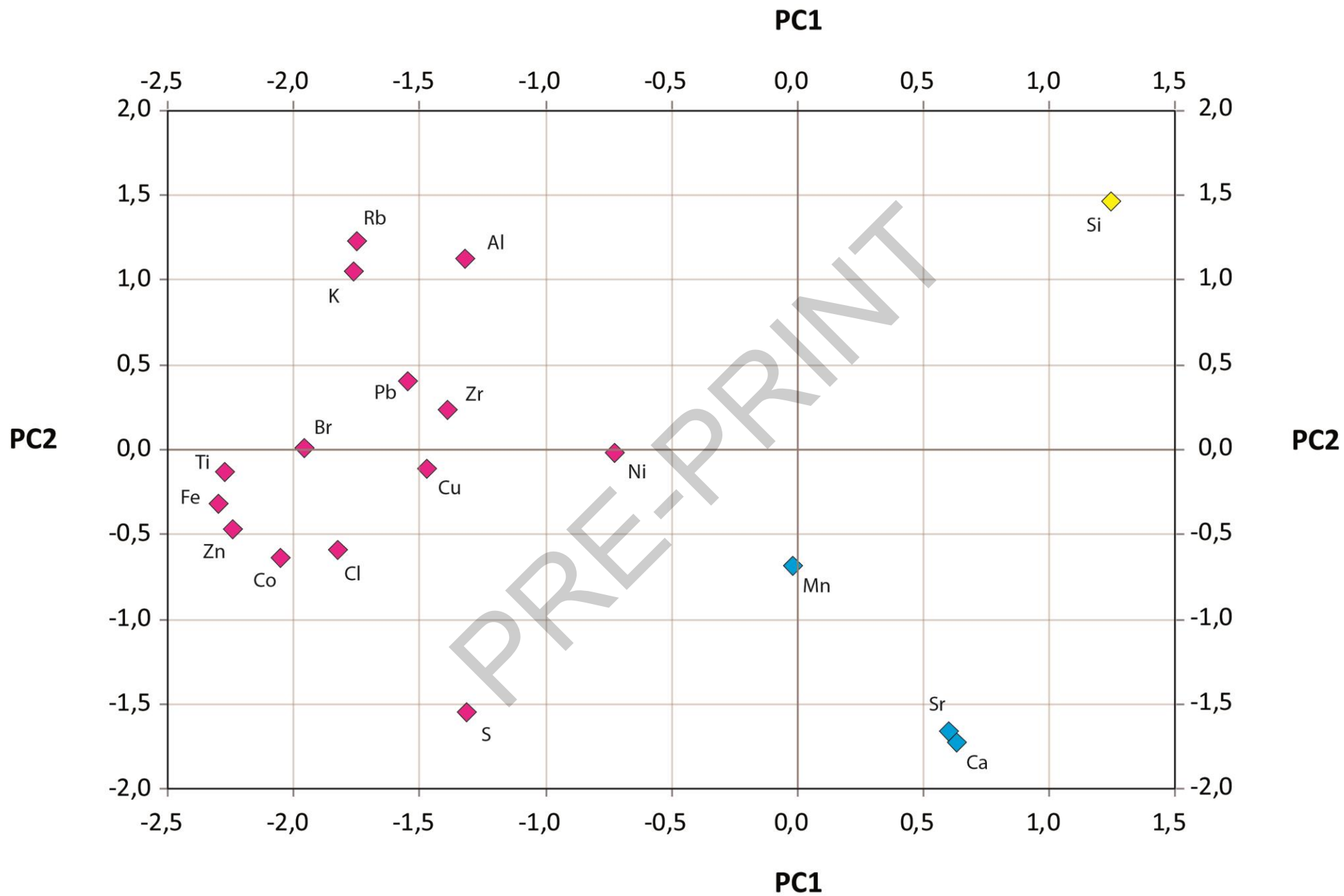
A. Traicts du Croisic (T1)



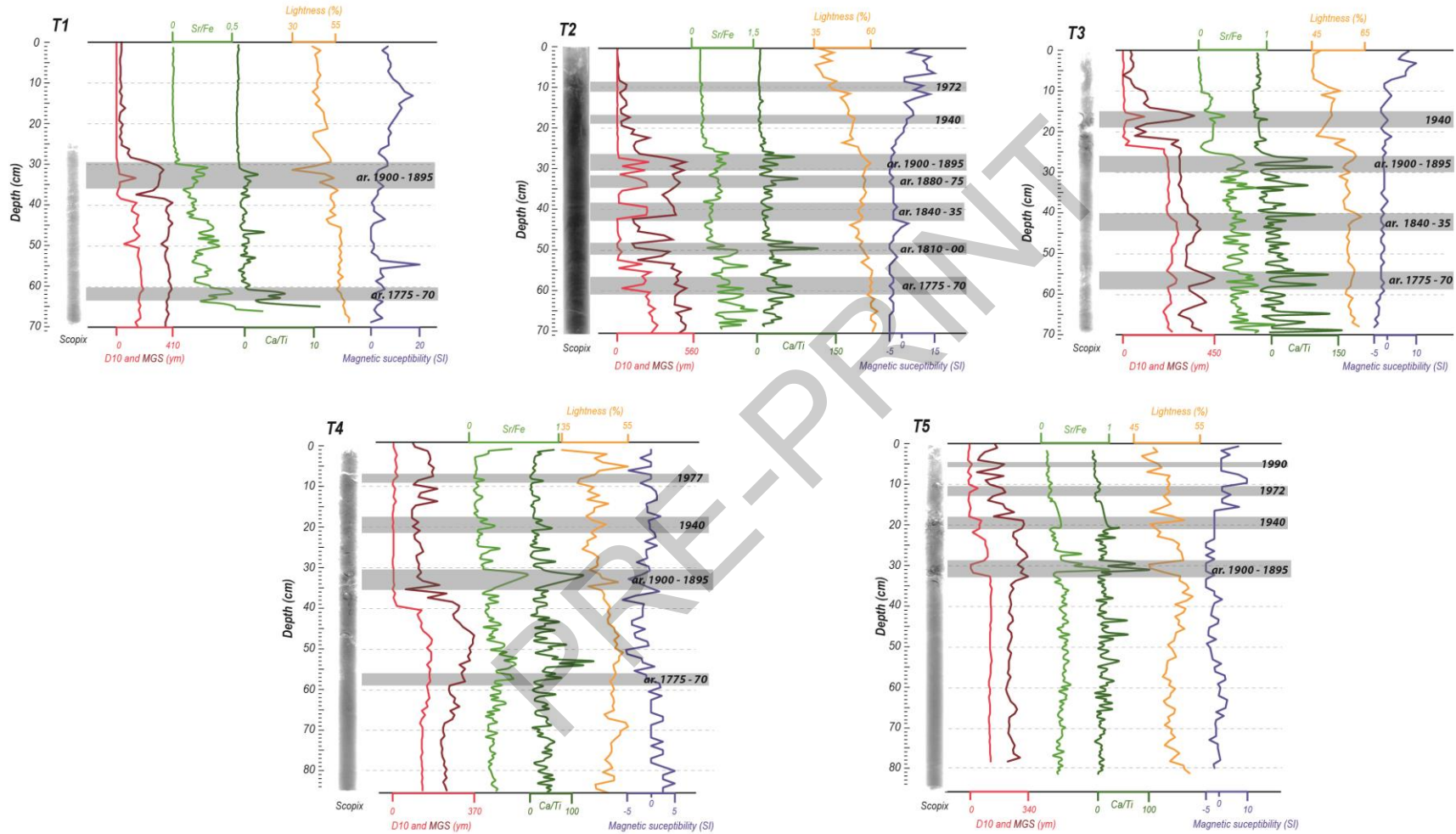
B. Petite mer de Gâvres (LB1)





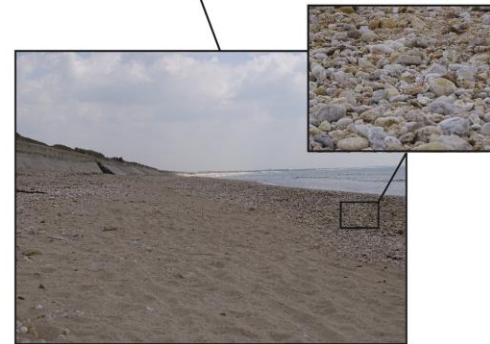
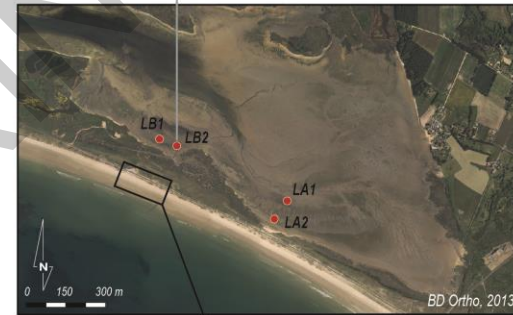
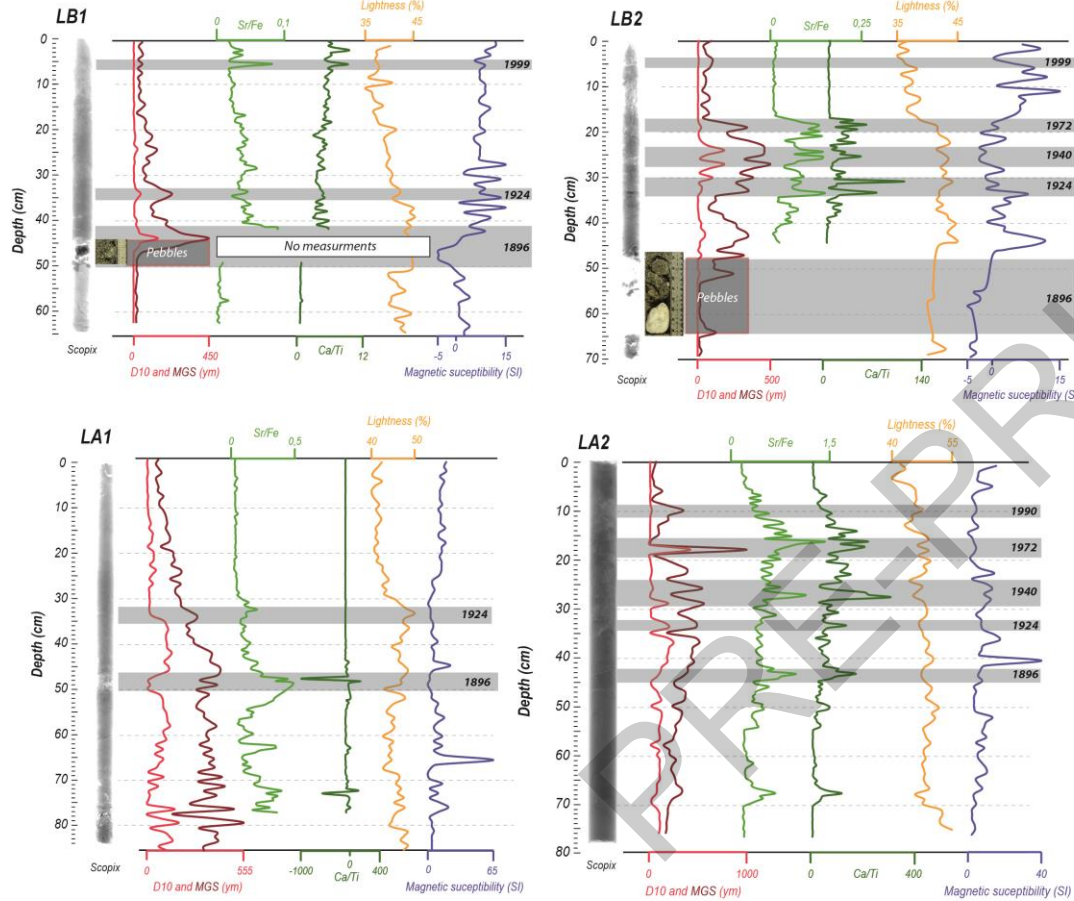


Pays-de-la-Loire region 1751 to 1999 marine flooding dates recorded in historical archives :
 1751 - 1760 - 1775 - 1811 - 1838 - 1876 - 1880 - 1884 - 1890 - 1896 - 1905 - 1924 - 1928 - 1934 - 1940 - 1972 - 1977 - 1987 - 1990 - 1999



1940 : Dates AD found with dating in sedimentological and historical archives for probable extreme wave event
 ar. 1775 - 70 : period estimated with the sedimentation rate for a probable extreme wave event (ar. : around)

Brittany region 1751 to 1999 marine flooding dates recorded in historical archives :
 1751 - 1760 - 1811 - 1876 - 1890 - 1896 - 1905 - 1924 - 1934 - 1940 - 1972 - 1987 - 1990 - 1999



1940 : Dates AD found with dating in sedimentological and historical archives for probable extreme wave event